Thermal Constriction Resistance of Sphere/Layered Flat Contacts: Theory and Experiment

N. J. Fisher
Chalk River Nuclear Laboratories,
Atomic Energy of Canada Limited,
Chalk River, Ontario, Canada

M. M. Yovanovich
UW Microelectronics Heat Transfer Laboratory,
Department of Mechanical Engineering,
University of Waterloo,
Waterloo, Ontario, Canada

The effect of surface layers on the thermal constriction resistance of contacts is of interest to the thermal analyst. This paper investigates analytically and experimentally the thermomechanical problem of a sphere in elastic contact with a flat coated with a layer. An approximate solution is developed that utilizes the solution to the thermal portion of the problem and the Hertzian limits of the mechanical portion. The approximation shows good agreement with the full solution for two examples that represent extremes in elastic properties for common metallics. Thermal constriction resistance measurements for a steel sphere contacting a nickel flat coated with a silver layer are compared to theoretical predictions. Resistance predictions from both full and approximate solutions show good agreement with measurements for light loads within the elastic load range. For heavy loads, the resistance is overpredicted due to plastic yielding of the nickel substrate.

Introduction

The use of surface layers within components is increasing as designers search for more variety and flexibility in material properties. Uses of layers include improving wear resistance, strength and corrosion resistance, modifying electrical and thermal conductivities, reducing weight, and conserving resources (Texas Instruments, 1983).

The development of computers with high chip densities makes efficient heat removal increasingly important. The Thermal Conduction Module (TCM), a key component of the IBM 3081 computer, is shown in Fig. 1 (Bar-Cohen et al., 1983). Each module contains an array of surface-mounted chips. The heat generated within each chip is removed through a spring-loaded aluminum piston, which presses onto the chip surface. A typical piston/chip contact is detailed in Fig. 2 (Chu et al., 1982). Heat transfer occurs through both the solid contact and the helium-filled gap. One technique to increase the heat removal rate is to add a thermally conductive layer to the piston/chip interface.

The purpose of this paper is to develop a simple model to predict the effect of a surface layer on the thermal constriction resistance of the piston/chip contact and to verify the model by comparing experimental resistance measurements to theoretical predictions.

Analysis

Idealized Model. The piston/chip contact is idealized as a nominal point contact between smooth surfaces, as shown in Fig. 3(*a*). The piston is modeled as a spherical indenter and the chip as a flat. Both bodies are idealized as half-spaces because the dimensions of the contact area are small as compared to the overall body dimensions. The indenter radius ρ_I is the reduced radius combining the radii of both bodies.

The addition of a layer to the piston/chip interface is modeled by including a layer on the flat, as shown in Fig. 3(*b*). This assumption does not restrict the applicability of the model. The layer can be added to either the piston or chip since both are assumed to be half-spaces in this analysis.

The complete model of the contact including the layer is shown in Fig. 4. The indenter (subscript *I*) is loaded onto a flat composed of a layer (subscript *L*) of thickness *t*, bonded to a substrate (subscript *S*).

In general, heat transfer can occur through both the contact and the surrounding gap. Heat transfer across the gap occurs by two different modes: conduction or convection, and radiation. The relative contributions of the two modes, for a gap size similar to this problem, have been investigated by Kitscha

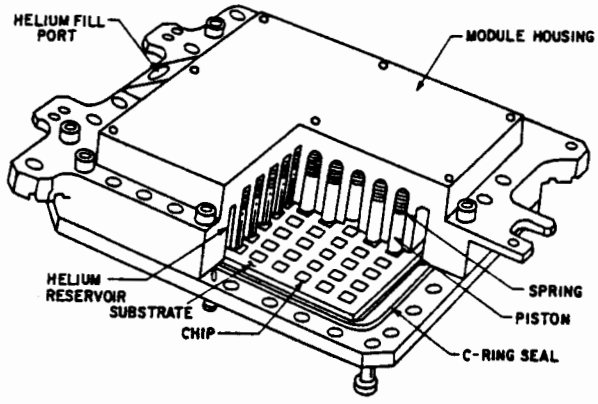

Fig. 1 Thermal conduction module

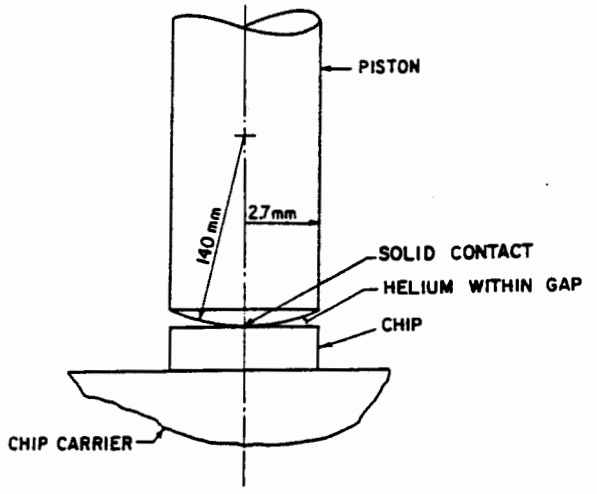

Fig. 2 Piston/chip contact

Contributed by the Heat Transfer Division and presented at the 4th AIAA/ASME Thermophysics and Heat Transfer Conference, Boston, Massachusetts, June 2–4, 1986. Manuscript received by the Heat Transfer Division November 30, 1987. Keywords: Conduction.

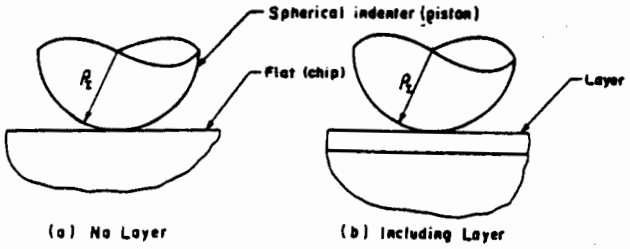

Fig. 3 Idealized piston/chip contact

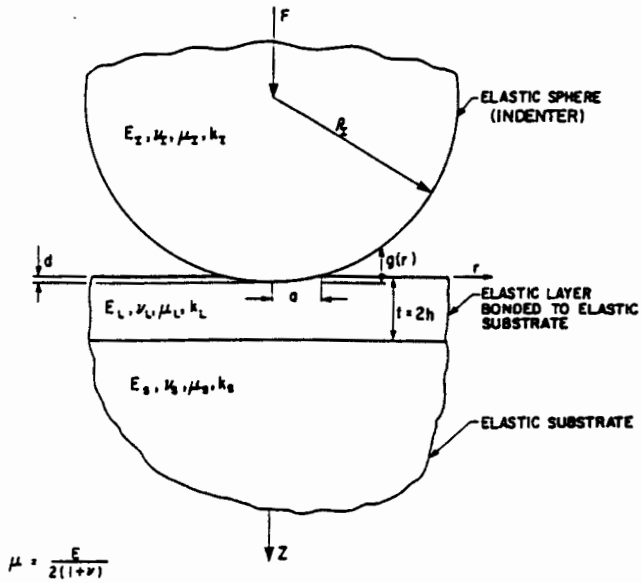

Fig. 4 Model of contact

and Yovanovich (1975), Ogniewicz and Yovanovich (1978), and Turyk and Yovanovich (1985).

Heat transfer by natural convection is found to be negligible. Models have been developed for conduction and radiation across the gap and, by comparison with experimental measurements for bare flats, these models have been shown to predict the heat transfer rate through the gap adequately.

The addition of a layer to the interface significantly affects the conductive heat transfer rate through the solid contact. Since the two heat transfer pathways (solid contact and gap) are coupled, changes in the temperature field and heat transfer rate across the solid contact will affect the temperature field and heat transfer rate across the gap. However, because this coupling is weak, the heat transfer rate through the gap is only slightly affected by the addition of a layer. Therefore, to simplify this analysis, heat transfer across the gap is neglected and only steady-state conduction heat transfer through the solid contact is considered.

The following assumptions further simplify the analysis: The mechanical and thermal properties of the bodies are assumed to be constant, the contact is assumed to form elastically, the bodies are assumed to be smooth with negligible surface roughness, the temperature drop across the contact is assumed to be small so thermal strain effects are negligible, and the heat flux distribution over the contact area is assumed to be equivalent isothermal, which is that flux distribution that results in an isothermal contact spot on a homogeneous half-space.

Analytical Solution. Heat flowing between the idealized bodies must flow through the solid contact area. The constriction and subsequent spreading of the heat flow lines gives rise to a thermal constriction resistance defined as the temperature difference across the contact divided by the total heat flow rate through the contact. This constriction resistance depends upon the load, geometry, and thermophysical properties of the contact.

The thermal constriction resistance for a sphere in elastic contact with a bare flat was investigated by Kitscha and Yovanovich (1975). They experimentally verified the analytical solution for the elastic load range. Antonetti and Yovanovich (1985) studied the problem of a rough conforming surface in contact with a smooth coated surface and developed an analytical solution for the constriction resistance, which they verified against experimental measurements.

The contact of a sphere and a flat consisting of a layer bonded to a substrate is a complicated problem. To predict the thermal constriction resistance of the contact, both mechanical and thermal portions of the problem must be solved. First, the mechanical portion is solved to find the radius a of the circular area of contact. Then, using the contact radius, the thermal portion is solved to find the constriction resistance.

The mechanical portion is a complex problem in axisymmetric elasticity governed by the following differential equation:

Nomenclature

a = contact radius
$\bar{a}$ = arithmetic average of bounding contact radii (equation (10))
d = approach or penetration
E = elastic modulus
F = load
$g(r)$ = indenter profile
h = layer half-thickness
H = hardness (Pa) or H_b (kg/mm^2)
k = thermal conductivity
m = mean asperity slope
r = radial coordinate
R = thermal constriction resistance
R^* = dimensionless resistance $= R\bar{a}k_s$
Q = heat flow rate
t = layer thickness
T = temperature
ΔT = contact temperature drop
z = axial coordinate
α = ratio of contact radius bounds (equation (6))
γ = ratio of reduced elastic moduli (equation (3))
κ = ratio of thermal conductivities (equation (3))
μ = shear modulus (Fig. 4)
ν = Poisson ratio
ρ = body radius
ρ_f = reduced radius (Fig. 4)
σ = rms surface roughness
τ = relative layer thickness (equation (3))
$\bar{\tau}$ = average relative layer thickness (equation (11))
ϕ = stress function
$\psi(\tau)$ = constriction parameter for an isothermal contact spot, Dryden's solution (equation (A1))

Superscripts

* = dimensionless or reduced
$\bar{}$ = average

Subscripts

AP = approximate solution
E = experimental measurement
I = indenter
L = layer
m = from measured plastic indentation
S = substrate

$$\nabla^2\nabla^2\phi=0 \tag{1}$$

where ϕ is the stress function (Timoshenko and Goodier, 1951) and ∇^2 is the Laplacian. The boundary condition is mixed, with the surface deflection prescribed within the contact area and the normal stress prescribed outside. For layered bodies, equation (1) cannot be solved to yield a closed-form solution for the contact radius. Instead, an iterative procedure is used in which an initial guess at the contact radius is continually updated until the calculated supported load equals the given load to some relative error criterion. Two solution procedures have been used to find the load supported by the contact of given radius.

With the integral transform method, the problem is formulated as a dual integral equation that is reduced to a Fredholm integral equation. The equation is then solved by expanding the kernel into a series of base functions. The shortcoming of the method is in the evaluation of the resulting integrals because they are slow to converge at the top surface of the layer near the boundary of the loaded region, especially for thin layers.

Chen and Engel (1972) circumvented this convergence difficulty with their general approximate method (GAM), in which they replaced the unknown stress condition within the contact area with an assumed set of base functions. The functions are assembled such that the displacement within the contact area approximates the real displacement boundary condition in accordance with an integral least-squares residual error criterion. The shortcoming of their method is that many numerical integrations are necessary to evaluate the displacement due to the assumed set of base functions.

The governing differential equation for the thermal portion is the Laplace equation

$$\nabla^2 T=0 \tag{2}$$

The boundary condition is mixed with the temperature prescribed within the contact area and the flux prescribed outside. Dryden (1983) removed the mixed boundary condition by replacing the unknown flux condition within the contact area with the equivalent isothermal flux distribution, which is the flux distribution that results in an isothermal contact spot on the surface of a homogeneous half-plane.

For thick layered half-spaces, $\tau \geq 10$, Negus et al. (1985) have shown that the equivalent isothermal flux condition is a good approximation to the true isothermal condition. However, for thin resistive layers, $\tau<1$ and $\kappa<1$, the uniform flux condition is a better approximation, while for thin conductive layers, $\tau<1$ and $\kappa>1$, the resistance due to the true isothermal condition is somewhat lower than the equivalent isothermal flux result and much lower than the uniform flux result. Application of Negus et al.'s superposition technique to this problem to solve for the true isothermal condition would be beneficial.

Dryden solved Laplace's equation using Hankel transforms to yield an integral expression for the constriction resistance, which he further simplified into simple closed-form expressions for the limiting cases of very thin and very thick layers and a series solution for intermediate layer thicknesses.

The combination of Chen and Engel's (1972) solution to the mechanical portion and Dryden's (1983) solution to the thermal portion forms a complete solution to the contact resistance problem of a spherical indenter contacting a layered, elastic half-space with an equivalent isothermal flux distribution over the contact area. As the layer thickness approaches zero, the resistance approaches that of an indenter contacting a half-space composed entirely of substrate material, and as the thickness approaches infinity, the resistance approaches that of an indenter contacting a half-space composed entirely of layer material. At these bounds, the equivalent isothermal distribution accurately represents the flux distribution for an isothermal contact. For intermediate layer thicknesses, the resistance predicted by this combined solution lies between these two bounding resistances.

Although the mechanical portion of the contact problem cannot be solved in closed form for layered bodies, a closed-form solution is available for the contact of unlayered bodies (Hertzian contact theory). By combining the Hertzian contact solution with Dryden's thermal solution, an approximate closed-form solution for the constriction resistance of the layered contact can be developed.

Resistance Bounds. Three important parameters influence the thermomechanical behavior of a flat composed of a layer bonded to a substrate (hereafter called a "layered flat"): ratio of elastic moduli γ, conductivity ratio κ, and relative layer thickness τ.

$$\gamma=\frac{E_L^*}{E_S^*} \qquad \kappa=\frac{k_L}{k_S} \qquad \tau=\frac{t}{a} \tag{3}$$

For a thin layer ($\tau \to 0$), the general layered contact reduces to the Hertzian contact of an indenter and a flat composed of substrate material. The contact radius a_S corresponding to the substrate bound is

$$a_S=\left[\frac{3}{4}\frac{F\rho_I}{E_S^*}\right]^{1/3} \tag{4}$$

where the reduced elastic modulus for the substrate bound E_S^* is

$$\frac{1}{E_S^*}=\frac{1-\nu_I^2}{E_I}+\frac{1-\nu_S^2}{E_S} \tag{5}$$

For a thick layer ($\tau \to \infty$), the general contact reduces to the Hertzian contact of an indenter and a flat composed of layer material. The contact radius a_L corresponding to the layer bound is

$$a_L=\left[\frac{3}{4}\frac{F\rho_I}{E_L^*}\right]^{1/3} \tag{6}$$

where the reduced elastic modulus for the layer bound E_L^* is

$$\frac{1}{E_L^*}=\frac{1-\nu_I^2}{E_I}+\frac{1-\nu_L^2}{E_L} \tag{7}$$

For all other values of τ, the contact radius a will lie between the two bounding radii, a_S and a_L. If the difference between the bounds is small, then they can be used to estimate the contact radius.

We define the ratio of the bounding radii α as

$$\alpha=\frac{a_L}{a_S} \tag{8}$$

Then α depends upon γ to the $-1/3$ power

$$\alpha=\gamma^{-1/3} \tag{9}$$

When γ is unity, the difference between the bounds is zero. As γ differs from unity, the difference between the bounds widens. For common metallics, the range of γ is

$$0.2 \leq \gamma \leq 5 \tag{10}$$

Therefore

$$1.7 \geq \alpha \geq 0.6 \tag{11}$$

or the bounding radii differ by less than a factor of two. For this condition, the arithmetic mean of the bounds $\bar{a}$ is a good estimate of the contact radius a

$$\bar{a} = \frac{a_S + a_L}{2} \tag{12}$$

and the average relative layer thickness $\bar{\tau}$ is a good estimate of the relative layer thickness τ

$$\bar{\tau} = \frac{t}{\bar{a}} \tag{13}$$

The harmonic and geometric means of the bounding radii were also examined as possible estimates of the contact radius. The three means differ by less than 3.5 percent for the particular case of $\gamma = 0.37$. Therefore, the arithmetic mean is arbitrarily chosen as a convenient estimate.

The total constriction resistance R of the system shown in Fig. 4 equals the sum of two constriction resistances in series: the resistance of an isothermal contact spot on the indenter and the resistance of an isothermal contact spot on the layered flat

$$R = \frac{1}{4a\,k_I} + \frac{\psi(\tau)}{4a\,k_S} \tag{14}$$

where the contact spot radius a must be calculated from the mechanical portion of the contact problem. The constriction parameter $\psi(\tau)$ for an isothermal contact spot on a layered flat is given by Dryden (1983).

The bounds on the constriction resistance, R_S and R_L, can be easily calculated from the bounding contact radii, a_S and a_L. The substrate resistance bound is

$$R_S = \frac{1}{4a_S k_I} + \frac{\psi(\tau_S)}{4a_S k_S}$$

where

$$\tau_S = \frac{t}{a_S} \tag{15}$$

and the layer resistance bound is

$$R_L = \frac{1}{4a_L k_I} + \frac{\psi(\tau_L)}{4a_L k_S}$$

where

$$\tau_L = \frac{t}{a_L} \tag{16}$$

Note that $\psi(\tau)$ is defined with respect to the substrate conductivity k_S (see Appendix).

Approximate Resistance. The bounding resistances approximate the constriction resistance of the system for small and large relative layer thicknesses. However, for intermediate layer thicknesses, the resistance lies between the bounds. For this range, an approximation combining the bounds is required.

For several layer-substrate combinations the dimensionless constriction resistance R^* was plotted versus the common logarithm of the average relative layer thickness $\bar{\tau}$. The dimensionless resistance is defined with respect to the average contact radius $\bar{a}$ and the substrate conductivity k_S

$$R^* = R\bar{a}k_S \tag{17}$$

The average contact radius is chosen as the nondimensionalizing length because it is load dependent and can be easily calculated from the bounding contact radii. The dimensionless bounding resistances are

$$R_S^* = \frac{\bar{a}}{4a_S}\left(\frac{k_S}{k_I} + \psi(\tau_S)\right) \tag{18}$$

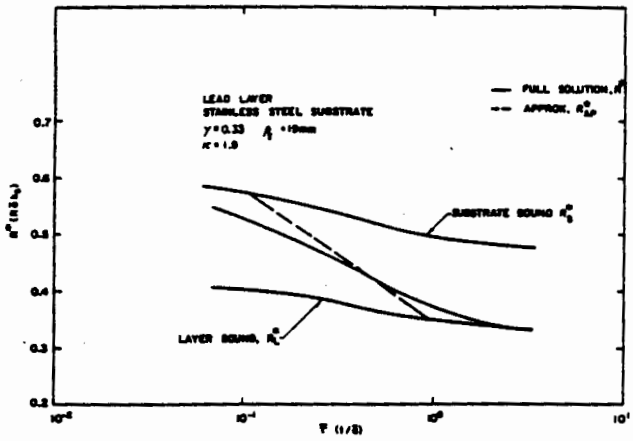

Fig. 5 R^* versus $\bar{\tau}$ for lead layer example

$$R_L^* = \frac{\bar{a}}{4a_L}\left(\frac{k_S}{k_I} + \psi(\tau_L)\right) \tag{19}$$

For the examined combinations, the following behavior was observed. For $\bar{\tau}$ less than 0.1, R^* approached the substrate bound, R_S^*, while for $\bar{\tau}$ greater than 1.0, R^* approached the layer bound R_L^*. Within the intermediate range, R^* varied logarithmically with $\bar{\tau}$. Therefore, the dimensionless resistance can be approximated as

$$R_{AP}^* = \begin{cases} R_S^* & \bar{\tau} \le 0.1 \\ R_{1.0}^* + (R_{1.0}^* - R_{0.1}^*)\log_{10}(\bar{\tau}) & 0.1 < \bar{\tau} < 1.0 \\ R_L^* & \bar{\tau} \ge 1.0 \end{cases} \tag{20}$$

where $R_{0.1}^*$ and $R_{1.0}^*$ are transition points defined as

$$R_{0.1}^* = \frac{\bar{a}}{4a_S}\left(\frac{k_S}{k_I} + \psi(0.1)\right) \tag{21}$$

$$R_{1.0}^* = \frac{\bar{a}}{4a_L}\left(\frac{k_S}{k_I} + \psi(1.0)\right) \tag{22}$$

In dimensional terms, the approximate resistance is

$$R_{AP} = \frac{R_{AP}^*}{\bar{a}\,k_S} \tag{23}$$

Analytical Results. The approximate dimensionless resistance R_{AP}^* is compared to the dimensionless resistance calculated using the full mechanical and thermal solutions R^* for two layer-substrate examples that represent relative extremes in elastic properties for common metallics.

The first example is a layered flat consisting of a lead layer on a stainless steel substrate in contact with a stainless steel sphere. The dimensionless parameters are $\gamma = 0.33$ and $\kappa = 1.9$, so the effect of the lead layer is to lower the constriction resistance. The dimensionless resistances are plotted versus $\bar{\tau}$ in Fig. 5.

The approximation overpredicts the resistance for $\bar{\tau}$ less than 0.5 and underpredicts for $\bar{\tau}$ greater than 0.5. The largest differences of 8 and -5 percent (relative to R^*) occur at the transition points $\bar{\tau} = 0.1$ and $\bar{\tau} = 1.0$, respectively, because the approximate resistance curve changes slope abruptly at these points, while the full solution curve changes slope gradually. The greater difference at the small transition point indicates that this transition point is less accurate. The approximation

Table 1 Properties of bare specimens

	Material	ρ_f, mm	E, GPa	ν	k, W/mK	σ, μm	Hardness
Flat 13A	Ni 200	∞	204	0.3	79.3	0.06	H_b* 103
Flat 15A	Keewatin TS	∞	204	0.3	33.5	<0.05	H_c† 60
Indenter (sphere)	Carbon Steel	38.1	207	0.3	45.7	<0.05	H_c 35

*H_b is Brinell hardness (kg/mm^2).
†H_c is Rockwell C hardness number.

Table 2 Properties of layered specimens

		Silver layer						Nickel substrate		
Test	t, μm	E, GPa	ν	k, W/mk	σ, μm	m	Hardness	E, GPa	ν	Hardness
14B	60	75	0.3	427	0.09	0.03	H_B* 65	204	0.3	H_b 103
14D	900	75	0.3	427	0.04	0.02	H_B 83	204	0.3	H_b 103

*H_B is Rockwell B hardness number.

would be improved for this example by shifting the small $\hat{t}$ transition point to $\hat{t}=0.05$.

The second example is a layered flat consisting of a chromium layer on an aluminum substrate in contact with an aluminum sphere. The dimensionless parameters are $\gamma=1.6$ and $\kappa=0.39$, so the chromium layer increases the constriction resistance. The dimensionless resistances are plotted versus $\hat{t}$ in Fig. 6.

The approximation underpredicts the resistance for $\hat{t}$ less than 0.12 and overpredicts for $\hat{t}$ greater than 0.12. The maximum difference of 5 percent occurs at $\hat{t}=0.2$. The small $\hat{t}$ transition point is again less accurate than the large $\hat{t}$ transition point. For this example the approximation would be improved by shifting the small $\hat{t}$ transition point to $\hat{t}=0.2$.

As noted in the two examples, the approximation could be improved by shifting the small $\hat{t}$ transition point. However, the position of this transition appears to depend on the relative properties of the particular layer/substrate combination. For the conductive layer, the recommended shift is toward smaller $\hat{t}$ and for the resistive layer, the shift is toward larger $\hat{t}$. The position of the transition point ($\hat{t}=0.1$) appears to be a reasonable compromise.

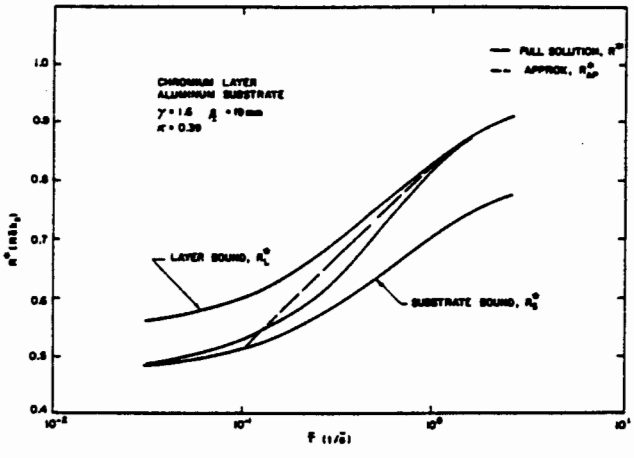

Fig. 6 R^* versus $\hat{t}$ for chromium layer example

Experiment

To verify the analytical models, an experimental test program was conducted to provide thermal constriction resistance measurements for comparison with theoretical predictions.

Apparatus and Procedure. A test column consisting of four sections was used in the experimental program: source, test, sphere, and sink. The source and sink specimens were heat flow meters, used to measure the heat flow rate above and below the contact. The temperature distributions within the test and sphere specimens were extrapolated to the contact plane to determine the temperature difference across the contact.

Axial loads were applied directly to the test column by a dead weight loading system, with a load range from 23.9 N to 688 N.

Heat was supplied to the column by a pair of resistive cartridge heaters positioned within the source specimen. The heat flowed axially down the column and was removed at the heat sink by a cold water bath. The column was wrapped in Fibrax insulation and aluminum foil to reduce heat losses in the radial direction.

Tests were conducted at a pressure less than 1×10^{-5} torr to eliminate convective and conductive heat transfer across the contact gap and radially, from the test column. The source and test specimens were maintained at temperatures below 373 K by using a low heat flow rate (approximately 1 W). In this manner, radiative heat transfer across the gap and radiative heat loss from the upper half of the test column were minimized. At this temperature level, the radiative heat flow rate across the gap was less than 1 percent of the total heat flow rate across the contact and could be neglected. The small temperature difference across the contact also reduced the effect of thermal strain at the sphere/flat interface.

To remove surface films, the sphere and test specimens were ultrasonically cleaned before each test in soapy deionized water and the contact surfaces were wiped with 1,1,1-trichloroethane ($C_2H_3Cl_3$) as recommended by Hegazy (1985).

Test specimens were fabricated from a single rod of commercially pure nickel (Nickel 200). The specimen for Test 15A was made from Keewatin Tool Steel. The ends of each specimen were ground and lapped smooth, and a silver layer was electroplated on one end. The layer surface was lapped smooth and uniform.

The properties of the bare flat specimens and the steel sphere are listed in Table 1. A smooth sphere was used so surface roughness effects could be neglected. The properties of the layered flat specimens are listed in Table 2. Handbook values (Baumeister, 1978) were used for the elastic modulus E, and Poisson ratio ν. The rms surface roughness σ, and mean asperity slope m, were measured with a surface profilometer.

Hardness values were measured for the bare and layered nickel flats using Brinell and Rockwell B hardness testers. Hardness values measured by McGee et al. (1985) and Kitscha and Yovanovich (1975) are listed for the bare Keewatin TS flat and the steel sphere. The layer thickness t was measured at the edge of the layered specimens by SEM. For one specimen, the thickness close to the contact spot was measured using eddy current techniques. The measurements from both techniques at both locations were of similar magnitude. X-ray energy spectroscopy of several layered specimens verified that the layer composition was at least 99 percent silver.

The temperature variation through each specimen was small. Consequently, the thermal conductivity was assumed uniform throughout each specimen, dependent only upon the average specimen temperature T. It was not possible to measure the conductivity of the thin silver layers, so the handbook value for pure silver at temperatures below 373 K was used (see Table 2).

The experimental contact resistance R_E was defined as the temperature difference across the contact ΔT divided by the heat flow rate through the contact Q

$$R_E = \frac{\Delta T}{Q} \tag{24}$$

The contact temperature difference was the difference in the extrapolated average contact plane temperatures, T_{e_1} and T_{e_2},

$$\Delta T = T_{e_1} - T_{e_2} \tag{25}$$

where T_{e_1} and T_{e_2} corresponded to the test specimen and sphere, respectively. These temperatures were calculated by extrapolating the specimen temperature distributions to the contact plane. For the layered specimens, the contact plane temperature T_{e_1} was assumed to equal the extrapolated temperature at the layer-substrate interface because the layer was thin and of high thermal conductivity. The interface resistance at the layer-substrate bond was neglected because the layer was deposited on a clean, smooth substrate. The resistance of this bond should be about two orders of magnitude less than the constriction resistance of the contact.

Heat flow rates were measured in both source and sink heat flow meters. The heat flow rate measured in the source was always greater than that measured in the sink since heat loss occurred along the test column. The sink heat flow rate was used to estimate Q since minimal heat loss occurred on the sink side of the contact (McGee et al., 1985). Equation (24) yields the conservative upper limit on the contact resistance because the sink heat flow rate is the minimum heat flow rate through the contact.

Experimental Results and Discussion

Bare Flats. Experiments were conducted with bare flats to establish the accuracy of the experimental procedure by comparison to the analytical model previously verified by Kitscha and Yovanovich (1975). Also, the bare nickel flat measurements (Test 13A) provided the upper bound on the constriction resistance for the subsequent tests with silver-nickel layered flats.

The theoretical resistance for the bare specimens is

$$R = \frac{1}{4k_f a} + \frac{1}{4k_s a} \tag{26}$$

If the contact behavior is elastic, the contact spot radius a can be calculated using Hertzian elastic theory

$$a = \left[\frac{3F\rho_f}{4E^*}\right]^{1/3} \tag{27}$$

where the reduced elastic modulus E^* is defined as

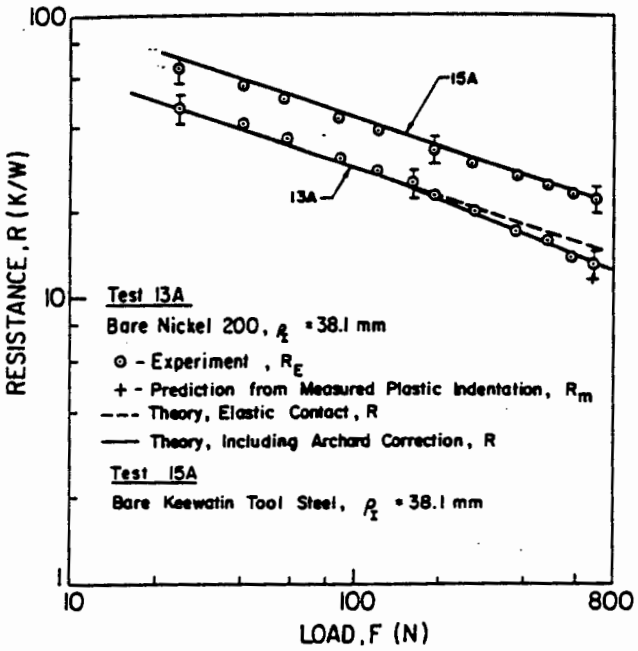

Fig. 7 Resistance versus load for bare flats

$$\frac{1}{E^*} = \frac{1-\nu_f^2}{E_f} + \frac{1-\nu_s^2}{E_s} \tag{28}$$

Experimental and theoretical resistances are plotted versus the applied load in Fig. 7 for the two tests with bare specimens: Nickel flat (13A) and Keewatin TS flat (15A). The probable experimental error in the measured resistance was ±8.5 percent and the probable error in the theoretical resistance due to uncertainty in the material properties is ±7 percent. The probable difference between the resistances is ±11 percent and this error bound is included on representative data points.

The agreement between the theoretical resistance based on Hertzian elastic theory and the experimental resistance is excellent for Test 15A. However, Hertzian theory overpredicts the measured resistance for the high load portion of Test 13A due to plastic deformation of the nickel flat. At the maximum load of 688 N, the experimental resistance is 14 percent less than the elastic theoretical prediction.

Archard (1980) developed a simple technique to estimate the load ranges for elastic and plastic contact behavior. The ranges of pure elastic and plastic behavior are defined in terms of the critical load F_c, where the elastic and plastic theories predict the same value for the contact radius

$$F_c = \frac{9\pi^3}{16} H^3 \left(\frac{\rho_f}{E^*}\right)^2 \tag{29}$$

The hardness H is the hardness of the softer material in pressure units. The three load ranges are:

$$\left.\begin{array}{ll} \text{(1) pure elastic} & F \le \frac{1}{15} F_c \\ \text{(2) elastic-plastic transition} & \frac{1}{15} F_c < F < 15 F_c \\ \text{(3) pure plastic} & F \ge 15 F_c \end{array}\right\} \tag{30}$$

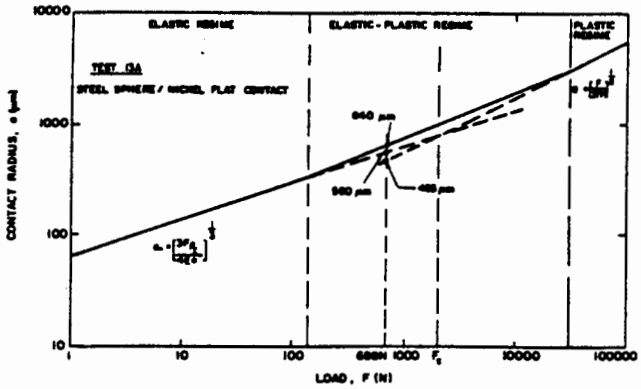

Fig. 8 Contact radius versus load: Nickel 200 flat

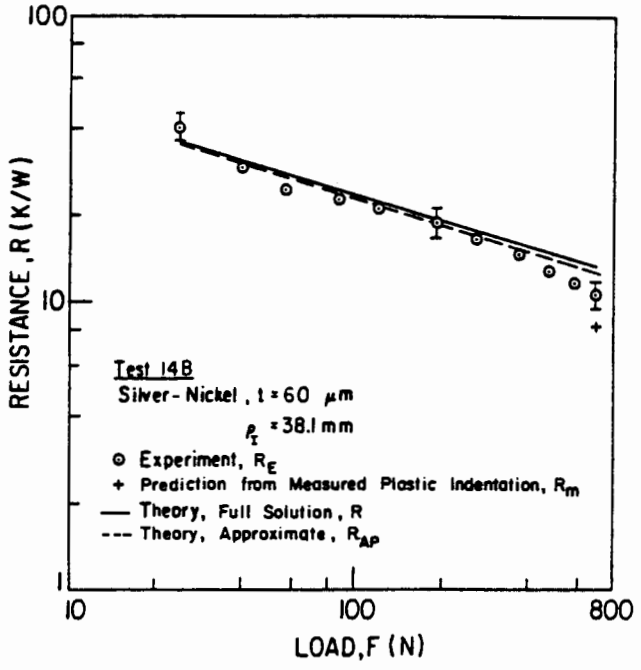

Fig. 9 Resistance versus load for silver-nickel flat; $t = 60$ μm

For Test 13A, the nickel flat is the softer material and determines the onset of plastic behavior. The critical load F_c is 2050 N and the elastic-plastic transition load range begins at 135 N. The onset of plastic behavior for Test 15A is controlled by the hardness of the steel sphere, which is softer than the Keewatin TS flat. For this test, F_c is 67.6 kN and the transition load range begins at 4500 N. After Test 13A, the nickel flat had an indentation of about 750 μm radius at the contact spot, but after Test 15A, neither the Keewatin TS flat nor the hardened steel sphere had any discernible plastic deformation.

The load range used in the experiments extended from 23.9 N to 688 N. Therefore, for Test 13A the contact behavior is elastic from 23.9 N to 135 N, and elastic-plastic from 135 N to 688 N. For Test 15A, the contact behavior is elastic for the full load range.

For loads greater than 135 N, the effect of elastic-plastic contact behavior must be included in the theoretical resistance predictions for Test 13A. The contact radius within the elastic-plastic load range is larger than predicted by either elastic or plastic theory. Archard (1980) recommended that simple curve fitting blending the theoretical curves for pure elastic and plastic deformation be used to estimate the contact radius within this range.

The theoretical curves for Test 13A are shown in Fig. 8. Within the elastic-plastic transition range, a straight line joining the elastic and plastic theoretical curves is chosen as a convenient estimate of the contact behavior. Actually, this estimate should provide the upper bound on the contact radius within this range. The extended curves for elastic and plastic deformation provide the lower bound for loads less than and greater than F_c, respectively.

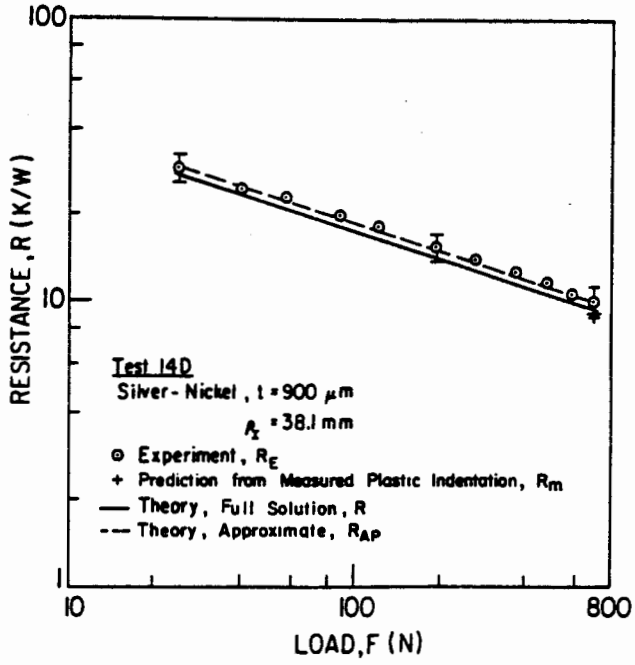

Fig. 10 Resistance versus load for silver-nickel flat; $t = 900$ μm

The theoretical curve including Archard's correction for elastic-plastic behavior is shown as the solid line on Fig. 7 for Test 13A. In the elastic-plastic load range, the agreement between this corrected prediction and the experimental resistance is excellent, with a maximum difference of 3 percent. The pure elastic curve is shown as a dashed line for loads greater than 135 N.

After each test the radius of the resulting plastic indentation, a_m, was measured. The predicted resistance R_m, calculated from a_m, is plotted with a plus (+) sign in Fig. 7.

Layered Flats. Nickel test specimens with silver layers of differing thickness were thermally tested in contact with a steel sphere. In Figs. 9 and 10, experimental resistances are compared to theoretical resistances predicted using the full solution: Chen and Engel's solution to the mechanical portion and Dryden's solution to the thermal portion. For Test 14B (Fig. 9) $\kappa = 5.4$ and $0.1 \le \tau \le 0.3$, while for Test 14D (Fig. 10) $\kappa = 5.4$ and $1.35 \le \tau \le 4.0$. The probable error bound (±11 percent) is included on representative data points. The theoretical resistance R_m, calculated using the measured plastic indentation a_m, is plotted with a plus (+) sign.

In general, the agreement between the theoretical and experimental resistances is good for the layered tests. For loads less than 135 N, the experimental data are in good agreement with the theoretical predictions. For loads greater than 135 N, the contact behavior for Test 14B (Fig. 9) is elastic-plastic due to plastic yielding of the softer nickel substrate (see Tables 1 and 2). Test 14D does not exhibit this behavior because the hard silver layer is relatively thick. The end of the pure elastic load range for Test 14B is consistent with the bare nickel test (13A), at approximately 135 N, verifying that the soft nickel substrate controls the onset of plastic deformation for this test.

Archard's elastic-plastic correction cannot be directly applied to the layered tests because the layer and substrate

materials have different hardness values. Antonetti and Yovanovich (1985) demonstrated that the contact theory for bare rough conforming surfaces is applicable to coated rough conforming surfaces if the effective hardness of the layer-substrate combination is used. The effective hardness is obtained from the hardness distribution for the particular combination. Therefore, to apply Archard's technique to the layered tests, it is suggested that the effective hardness of the silver/nickel combination be used to predict the critical load. To estimate the elastic-plastic contact radius for a given load, several iterations would be required since the effective hardness and contact radius are interrelated.

Conclusions

A simple analytical model has been developed to approximate the thermal constriction resistance of a sphere in elastic contact with a layered flat. The approximation utilizes the limiting cases of the mechanical portion of the contact problem incorporated with Dryden's solution to the thermal portion. For two examples representing relative extremes in elastic properties for common metallics, the approximation compares favorably to results obtained using the full mechanical and thermal solutions to calculate the constriction resistance.

The analytical models have been verified by comparing experimental resistance measurements to theoretical predictions.

Two different bare flats were tested in contact with a steel sphere: Nickel 200 and Keewatin TS. Excellent agreement is observed between the experimental resistances and theoretical predictions for light loads within the elastic load range. For the nickel test, elastic theory overpredicts the measured resistance at heavy loads due to plastic deformation of the nickel flat. With the theoretical predictions corrected for elastic-plastic contact behavior, excellent agreement between experiment and theory is obtained for the full load range.

Two nickel test specimens with silver layers of different thickness were tested in contact with a steel sphere. Good agreement is observed between the experimental measurements and theoretical predictions for light loads. For heavy loads, elastic theory overpredicts the resistance due to plastic deformation of the nickel substrate. It is suggested that the technique used to correct for elastic-plastic behavior of the bare nickel contact could be applied to the layered contact by introducing the effective hardness of the layer/substrate combination.

Acknowledgments

The authors acknowledge R. Kaptein for technical assistance with the design of the experimental apparatus, A. Hodgson for fabrication of experimental hardware, A. Hegazy for surface roughness measurements, and C. Lane for thermal measurements in Test 15A. N. J. Fisher acknowledges financial support received under the Natural Sciences and Engineering Research Council of Canada Postgraduate Scholarship and the Ontario Graduate Scholarship.

References

Antonetti, V. W., and Yovanovich, M. M., 1985, "Enhancement of Thermal Contact Conductance by Metallic Coatings: Theory and Experiment," ASME JOURNAL OF HEAT TRANSFER, Vol. 107, pp. 513–519.

Archard, J. F., 1980, "Wear Theory and Mechanisms," *Wear Control Handbook*, M. B. Peterson and W. O. Winer, eds., ASME, New York, pp.35–80.

Bar-Cohen, A., Kraus, A. D., and Davidson, S. F., 1983, "Thermal Frontiers in the Design and Packaging of Microelectronic Equipment," *Mechanical Engineering*, pp. 53–59.

Baumeister, T., 1978, *Marks' Standard Handbook for Mechanical Engineers*, 8th ed., McGraw-Hill, New York.

Chen, W. T., and Engel, P. A., 1972, "Impact and Contact Stress Analysis in Multilayer Media," *Int. J. Solids Structures*, Vol. 8, pp. 1257–1281.

Chu, R. C., Hwang, U. P., and Simons, R. E., 1982, "Conduction Cooling for an LSI Package: A One-Dimensional Approach," *IBM J. Res. Develop.*, Vol. 26, No. 1, pp. 45–54.

Dryden, J. R., 1983, "The Effect of a Surface Coating on the Constriction Resistance of a Spot on an Infinite Half Plane," ASME JOURNAL OF HEAT TRANSFER, Vol. 105, No. 2, pp. 408–410.

Hegazy, A. A., 1985, "Thermal Joint Conductance of Conforming Rough Surfaces: Effect of Surface Micro-Hardness Variation," Ph.D. Thesis, University of Waterloo, Canada.

Incropera, F. P., and DeWitt, D. P., 1981, *Fundamentals of Heat Transfer*, Wiley, New York.

Kitscha, W. W., and Yovanovich, M. M., 1975, "Experimental Investigation on the Overall Thermal Resistance of Sphere-Flat Contacts," *Heat Transfer With Thermal Control Applications*, M. M. Yovanovich, ed., Vol. 39, Progress in Astronautics and Aeronautics, AIAA, MIT Press, Cambridge, MA, pp. 93–110.

Negus, K. J., Yovanovich, M. M., and Thompson, J. C., 1985, "Thermal Constriction Resistance of Circular Contacts on Coated Surfaces: Effect of Contact Boundary Conditions," AIAA85-1014, 20th Thermophysics Conference, Williamsburg, VA; accepted for publication in *Journal of Thermophysics and Heat Transfer*.

McGee, G. R., Schankula, M. H., and Yovanovich, M. M., 1985, "Thermal Resistance of Cylinder-Flat Contacts: Theoretical Analysis and Experimental Verification of a Line-Contact Model," *Nuclear Engineering and Design*, Vol. 86, pp. 369–381.

Ogniewicz, Y., and Yovanovich, M. M., 1978, "Effective Conductivity of Regularly Packed Spheres: Basic Cell Model With Constriction," *Heat Transfer and Thermal Control Systems*, L. S. Fletcher, ed., Vol. 60, Progress in Astronautics and Aeronautics, AIAA, New York, pp. 209–228.

Texas Instruments, 1983, "TI Clad Metals."

Timoshenko, S., and Goodier, J. N., 1951, *Theory of Elasticity*, 2nd ed., McGraw-Hill, New York.

Turyk, P. J., and Yovanovich, M. M., 1985, "Modified Effective Conductivity Models for Basic Cells of Simple Cubic Packed Beds," *Heat Transfer in Porous Media and Particulate Flows*, HTD-Vol. 46, ASME, New York, pp. 9–19.

APPENDIX

Constriction Parameter for a Layered Half-Space

The constriction parameter $\psi(\tau)$ is defined in terms of the substrate thermal conductivity k_S, and is dependent upon the relative layer thickness τ and the conductivity ratio κ

$$\psi(\tau) = 4k_S aR \tag{A1}$$

Dryden (1983) reports expressions for three different ranges of relative layer thickness. For thin layers ($\tau \le 0.01$), a linear approximation is given

$$\psi(\tau) = 1 + \frac{4\tau}{\pi\kappa}(1-\kappa^2), \qquad \tau \le 0.01 \tag{A2}$$

and for thick layers ($\tau \ge 2$), a logarithmic approximation is provided

$$\psi(\tau) = \frac{1}{\kappa} - \frac{2}{\pi\tau\kappa}\ln\left(\frac{2}{1+\kappa}\right), \qquad \tau \ge 2 \tag{A3}$$

For intermediate layer thicknesses ($0.01 < \tau < 2$), Dryden presents a series solution

$$\psi(\tau) = 1 + \frac{4\tau}{\pi\kappa}(1-\kappa^2) + \frac{8}{\pi\kappa}\sum_{j=1}^{\infty}\left[\frac{\kappa-1}{\kappa+1}\right]^j N(\theta_j), \qquad 0.01 < \tau < 2 \tag{A4}$$

where

$$N(\theta_j) = \left[1-e^{-2\phi}\right]^{1/2}\left[e^{\phi} - \frac{e^{-\phi}}{2}\right] + \frac{1}{2}\sin^{-1}(e^{-\phi}) - \frac{\pi}{4} \tag{A5}$$

$$\phi = \ln\left(\frac{\theta_j}{2} + \left[\frac{\theta_j^2}{4}+1\right]^{1/2}\right) \tag{A6}$$

$$\phi_j = 2j\tau \tag{A7}$$